RESONANT TUNNELING IN SEMICONDUCTOR HETEROSTRUCTURES

E. Mendez

JOURNAL DE PHYSIQUE
Colloque C5, supplément au n°11, Tome 48, novembre 1987

RESONANT TUNNELING IN SEMICONDUCTOR HETEROSTRUCTURES

E.E. MENDEZ

IBM Thomas J. Watson Research Center, Yorktown Heights, NY 10598, U.S.A.

Abstract- This paper reviews some of the recent advances in resonant tunneling in GaAlAs-GaAs-GaAlAs heterostructures. The emphasis is on new physical mechanisms that enlarge the simple picture of one-dimensional, single-band, tunneling in semiconductors. I discuss the effect of a strong magnetic field and of hydrostatic pressure on resonant tunneling, and then I consider X-state resonant tunneling in addition to tunneling via states derived from a Γ-point potential profile. The limitations of our current understanding of these processes are pointed out.

1. Introduction

In semiconductor heterostructures, the motion of electrons perpendicular to the interfaces is governed by the potential determined by the conduction-band edges of the materials. If a semiconductor has a band edge higher in energy than the one from which the electron originates, transport takes place via tunneling. Resonant tunneling results at certain energies, from the constructive interference between incident and reflected waves at a potential discontinuity. This general quantum-mechanical concept was applied to metal-insulator-metal structures [1], and metal-insulator-semiconductor-insulator-metal heterolayers [2]. In both cases, the metal electrodes would provide a range of electron energies up to the Fermi level and the resonance conditions would be achieved under certain voltages applied between them.

The first experimental confirmation of resonant tunneling via quantum states was provided by Chang, Esaki and Tsu [3], who used GaAs as the intermediate semiconductor, $Ga_{0.30}Al_{0.70}As$ as the insulator, and n^+-GaAs electrodes instead of the end metals. The current-voltage characteristics of those heterostructures showed weak negative-resistance features, interpreted as tunneling between the electrodes through states in the GaAs quantum well. The voltages corresponding to negative resistance, $V_{i,res}$, were directly related to the quantum-state energies, E_i, and in an ideal symmetric system it would be $eV_{i,res} = 2E_i$, where e is the electronic charge.

Substantial advances in materials preparation have led to stronger negative-resistance structures [4] and have made it possible the observation of new, related, effects. Thus, Mendez et al. [5] have reported resonant tunneling of holes in AlAs-GaAs-AlAs heterolayers sandwiched between p^+-GaAs electrodes. Because of tunneling of both light and heavy holes, the picture is more complicated than in the case of electrons and the identification of both sets has required a temperature-dependence study.

Resonant tunneling has been observed not only in single-quantum-well heterostructures but also in double-well structures, whenever the applied bias makes states in one well coincident with those in the other [6,7], and in multiple wells, by sequential tunneling between quantum states [8]. The trend towards a larger number of wells has its ultimate expression in resonant tunneling in superlattices, studied by Esaki and Chang [9] and more recently by Davies et al. [10].

The initial resonant-tunneling observations in GaAs-GaAlAs have been extended to other systems, such as GaAsP-GaP [11], InGaAs-InP [12], and even HgTe-HdCdTe [13]. Part of the interest in resonant tunneling stems from the possibility of using the negative-resistance effects in high-speed devices. In addition to two-terminal applications developed by Sollner et al. [4,14], novel three-terminal structures have been proposed and some have been already demonstrated [15,16].

In this paper, I will review our recent work on resonant tunneling, emphasizing its physical implications. I will focus on resonant magnetotunneling [17], on the effect of hydrostatic pressure on tunneling, particularly in those structures where the GaAlAs barrier is near the direct-indirect band-gap transition [18], and on resonant tunneling via X-point states [19,20]. The material structures discussed here consist of $Ga_{1-x}Al_xAs$-GaAs-$Ga_{1-x}Al_xAs$ $(0.3 \leq x \leq 1)$ double-barrier heterolayers, clad between either n^+- or p^+-electrodes, and grown by molecular beam epitaxy on GaAs substrates oriented along the (100) direction.

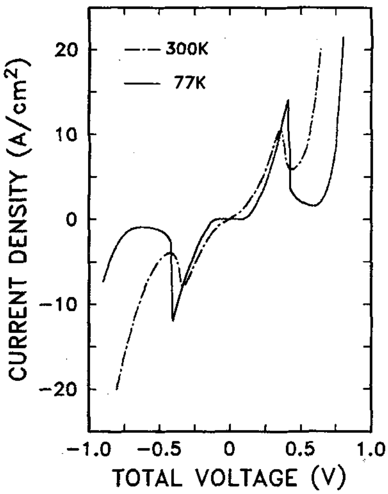

Fig.1.- Current-voltage characteristics of a GaAs-$Ga_{0.47}Al_{0.53}As$ double-barrier heterostructure (DBH), clad between n^+ electrodes, at 300K and 77K. The layer widths were 50Å. The negative-resistance voltage is directly related to the energy of the quantum state in GaAs.

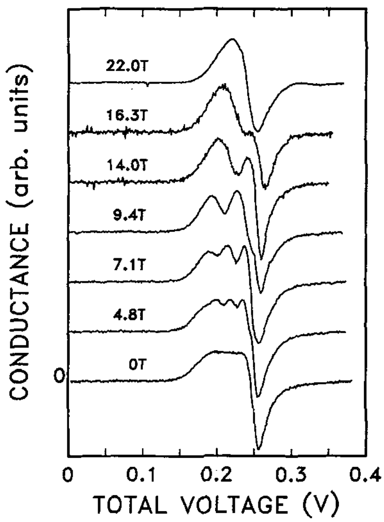

Fig.2.- Resonant tunneling of electrons in a magnetic field parallel to the current. The figure shows the conductance at 4K vs applied bias for a GaAs-$Ga_{0.60}Al_{0.40}As$ DBH. The thicknesses of the well and barriers were 40Å and 100Å, respectively. (After Ref. [17].)

Figure 1 shows the current-voltage (I-V) characteristics of a typical heterostructure, at room temperature and 77K. At low temperature and moderate voltages, the current is determined only by tunneling processes. At very low bias, the current is negligible, until the voltage is such that the energy of the quantum state coincides with the Fermi energy of one of the electrodes. At this point resonant tunneling proceeds, with the current increasing linearly with voltage until the quantum state is below the conduction-band edge of the electrode. From then on, conservation of momentum parallel to the interface forbids resonant tunneling and the current drops drastically. In this view, the I-V characteristic should have a triangular shape, and for symmetric barriers the voltage width would be twice the electrode Fermi energy.

Ideally, the peak current would be several orders of magnitude larger than the minimum current beyond resonance. Although this ratio has increased steadily over the years as the materials quality has improved, it is still of the order of ten to twenty, in the best devices. Thus, for the sample of Fig.1 it is ~13 at 77K and ~14 at 4K. The big discrepancy between calculated and experimental peak-to-valley ratios suggests additional mechanisms to the tunneling current, possibly non-conserving momentum processes, that need further consideration. However, in spite of its simplicity, this model of tunneling can explain to first order the lineshape of the I-V characteristics and in some cases even the peak current densities.

2. Resonant Magnetotunneling

In the presence of a strong magnetic field applied parallel to the tunneling current, the I-V characteristic shows features in its positive-slope region that approach the form of plateaus at fields of ~15-20T. These features are better resolved in conductance measurements, as shown on Fig.2 for a 100Å-40Å-100Å heterostructure with $Ga_{0.60}Al_{0.40}As$ barriers, clad between n^+ contacts.

At zero magnetic field, the shape of the conductance, with a flat region followed by a sharp drop to negative values, corresponds to a quasi-triangular I-V characteristic. For fields above 3T, conductance oscillations are visible at voltages below the negative conductance. Their amplitudes increase with field, and their positions shift to higher bias until they merge with the principal, field-independent, conductance minimum. If the magnetic field is applied perpendicularly to the current none of these effects are present, but the zero-field negative resistance gradually disappears as a result of the change in momentum along the current direction induced by the magnetic field.

The conductance oscillations, and correspondingly the quasi-plateaus of the current, can be explained in terms of resonant tunneling via Landau levels. In a magnetic field, B, parallel to the current, the motion of the electrons is quantized in the interface plane, and produces Landau states with energies given by $(N + 1/2)\hbar\omega_c$, where N is the level index (N=0,1,2,...), $\omega_c = eB/m^*$ is the cyclotron frequency, and m^* is the electronic effective mass. (For simplicity, we have ignored spin and have assumed that the effective mass in the electrodes is the same as in the quantum well.) At the electrode the electrons can move freely along the field direction, and therefore we can talk of Landau subbands. On the other hand, in the well the motion is fully quantized and the density of states in it can be seen as a series of broadened δ functions peaked at the Landau-level energies.

As a bias is applied, the N=0 peak goes down in energy relative to the low-voltage electrode and eventually is aligned with the Fermi level (which, to first approximation, does not change with B). Then, electrons from the electrode in the N=0 state can tunnel via the same Landau level of the well and the current increases. As the density-of-states peak drops below the Fermi energy, the current remains constant until the next state, N=1, coincides with the Fermi level and then it increases again, while conserving Landau index. The process continues with a series of rises and plateaus in the current until the Landau levels of the well are aligned with the bottoms of the corresponding subbands of the electrode. Beyond that voltage tunneling is forbidden and the current suddenly stops.

The effects induced by the field give rise to oscillations in the conductance, as seen on Fig.2. The conductance should have a minimum (and ideally would be zero) at voltages V_{min} such that

$$eV_{min} = E_0 - E_F + (N + 1)\hbar\omega_c. \qquad [1]$$

Alternatively, for fixed bias, the conductance shows analogous oscillations as a function of the magnetic field. A fit of the experimental voltages to Eq.[1] yields the electron effective mass in the well and the Fermi energy at the electrode. For the case shown on Fig. 2 those values were $0.063m_0$ (m_0 is the free-electron mass) and 0.041 eV, respectively. The mass value is slightly smaller than the one normally accepted for GaAs, especially after taking non-parabolicity effects into account. As pointed out by Goldman and Tsui [21], the discrepancy is probably due to the fact that part of the voltage drops outside the double-barrier region, a correction that was not included in the data analysis.

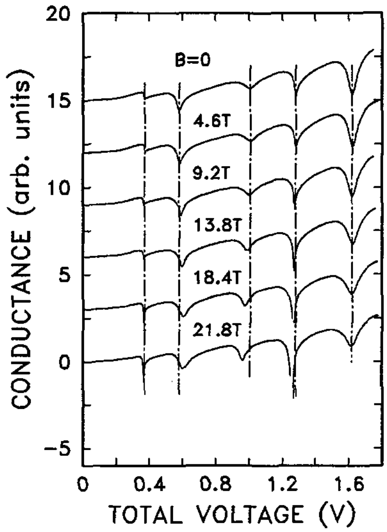

Fig.3.- Resonant tunneling of holes, at 0.5K, in a magnetic field parallel to the tunneling direction. The plot shows the conductance vs voltage for a GaAs-AlAs DBH, with 50Å layer widths. The dotted lines are guides to the eye, to illustrate the field-induced shifts of some of the negative-resistance structures. (After Ref.[5].)

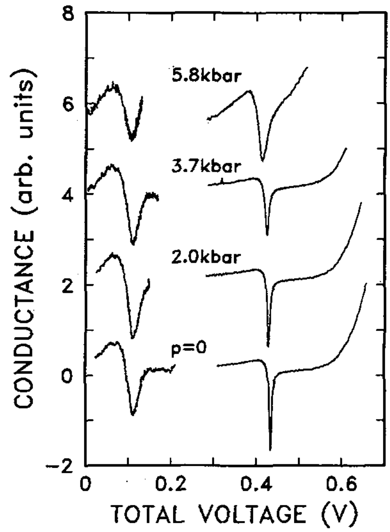

Fig.4.- Effect of hydrostatic pressure on the negative-resistance structures of a GaAs-$Ga_{1-x}Al_xAs$ DBH (x=0.40), at 77K. The widths of the barriers were 100Å, and that of the well was 60Å With increasing pressure, the structures shift monotonically to lower voltages, and become weaker. Above 8.5 kbar they are not well resolved.

The effect of the field on the negative-resistance structure itself is seen to be very small. However, if the difference of effective masses between the electrode and the quantum well were significant, a field-induced shift could be noticeable, which would be either positive or negative, depending on the sign of the mass difference. This situation is realized in the case of resonant tunneling of holes, illustrated on Fig.3. In the presence of a strong magnetic field some of the zero-field minima shift to lower voltage, others to higher voltage, and still some remain unshifted. In spite of the strong valence-band mixing, these results can be interpreted in terms of resonant tunneling of heavy and light holes from the electrode via heavy- and light-hole quantum states. Of all possible combinations between initial and well states, the heavy-to-light tunneling will suffer an upshift, while the light-to-heavy one will be downshifted.

Surprisingly, none of the oscillatory structures seen in the case of electrons is observable for holes, even up to 30T. This absence, as well as the lack of any spin effects in electron tunneling, requires further study. Another point that deserves more consideration is the Landau-level conservation rule, since, some samples show at very high fields weak additional minima beyond the negative-resistance structure, suggesting a possible breakdown of that conservation law.

3. Effect of Hydrostatic Pressure on Resonant Tunneling

Since the resonant tunneling voltage gives direct information on the bound states of the quantum well, and those in turn depend on the barrier height, it is not surprising that hydrostatic pressure measurements have been able to provide values for the pressure coefficient of the conduction-band discontinuity between GaAs and $Ga_{0.60}Al_{0.40}As$ [18]. Even more important is the conclusion reached from those experiments that resonant tunneling is determined by a potential profile that preserves symmetry, while nonresonant tunneling occurs preferentially through the lowest potential barrier.

The high-pressure measurements (up to 11kbar) were done at 77K, on $Ga_{0.60}Al_{0.40}As$-GaAs-$Ga_{0.60}Al_{0.40}As$ heterostructures clad between n^+-GaAs contacts. The $Ga_{1-x}Al_xAs$ barriers were 100Å wide and the GaAs well was either 40Å or 60Å thick. Figure 4 shows the conductance for the 60Å-well sample at representative pressures, up to 6kbar. The two negative-resistance structures correspond to the two bound states in the well. As the pressure increases, the minima shift to lower bias and their intensities decrease until eventually they disappear at the highest pressure.

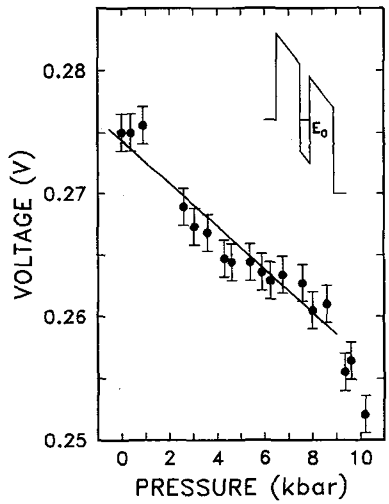

Fig.5.- Voltage of minimum conductance for a GaAs-GaAlAs DBH (x=0.40) with a 40Å well and 100Å barriers, as a function of hydrostatic pressure. The voltage shift is directly related to the change in energy of the bound state E_0, and this, in turn, to the decrease of the barrier height with increasing pressure. (After Ref.[18].)

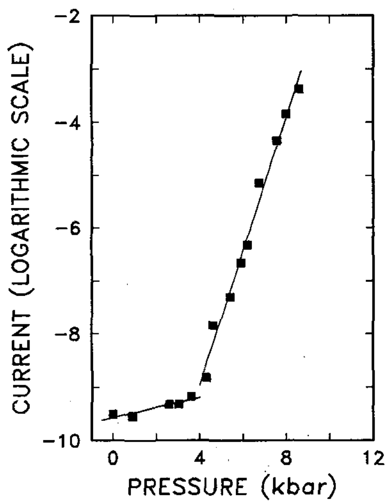

Fig.6.- Natural logarithm of the tunneling current at high bias (0.55V) vs pressure, for the same heterostructure as in Fig.5. The sharp change in the slope at p~4 kbar corresponds to the pressure at which the Γ and X points of $Ga_{0.60}Al_{0.40}As$ have the same energy. At higher pressures, X is lower in energy than Γ. (After Ref.[18].)

The voltage of minimum conductance, for the 40Å sample, is plotted in Fig.5. The monotonic shift arises in part from a pressure-induced increase in the effective mass, but mostly from a reduction of the barrier height. As the mass scales with the energy gap (whose pressure coefficient is well known) the decrease of barrier height with pressure can be deduced from the change in energy of the quantum state E_0. An analysis of Fig.5 yields a reduction of the potential barrier of ~3meV/kbar. It should be noted that the E_0 shift is smooth at least until 8.5kbar, beyond which pressure the minimum in conductance is not well defined. The absence of any discontinuity in the shift rate in the range 4-5kbar, which is the pressure at which $Ga_{0.60}Al_{0.40}As$ becomes indirect, demonstrates that E_0 is determined solely by the Γ-Γ potential, independently that the Γ point may be higher in energy than the X point.

The non-resonant tunneling current behaves quite differently. At voltages above the negative-resistance feature, the current increases moderately up to 4kbar, but then it presents an abrupt rise, as seen on Fig.6. The initial increase is consistent with the reduction of the Γ-Γ potential barrier discussed above. Indeed, an analysis of the slope yields a barrier decrease of ~1.7meV [18], in reasonable agreement with the 3meV/kbar value. However, the rapid rise above 4kbar requires a different explanation. Since this is the pressure at which the X and Γ point of $Ga_{0.60}Al_{0.40}As$ have approximately the same energy, and at higher pressure X drops relative to Γ at a rate of ~12meV/kbar, the abrupt change shows that the minimum potential barrier, irrespectively of symmetry, can be important in determining the total tunneling current.

The effective mass for electron tunneling through the Γ-X barrier can be determined from the rate of current increase, once the pressure coefficient is known [18]. A simple analysis using the WKB approximation in the Fowler-Nordheim regime yields a mass value of ~$0.18m_0$, in good agreement with data available in the literature for the transverse mass of the [010] and [001] X ellipsoids, X_y and X_z , respectively [22]. These tunneling paths do not conserve momentum parallel to the interfaces, and, in principle they could be less likely than the momentum-conserving paths. Therefore, there might be situations, depending on the transfer rate as well as the thickness of the barriers, in which the latter might dominate over the former, even when Γ-Γ is significantly higher than Γ-X.

4. Resonant Tunneling via X states

Although tunneling from Γ electrons in GaAs through X in $Ga_{1-x}Al_xAs$ does not conserve momentum for two of the X-point ellipsoids, momentum parallel to the interface is conserved if tunneling occurs via the [100] ellipsoid. Moreover, since the energy of the X point decreases with increasing x, it follows that in a potential profile derived from X, $Ga_{1-x}Al_xAs$ acts as a confining well for electrons, separated by GaAs barriers. It is then possible for Γ electrons to tunnel resonantly via X-point quantum states localized in $Ga_{1-x}Al_xAs$.

The existence of these states has been demonstrated in optical measurements by Finkman et al., in GaAs-AlAs quantum wells [23]. The experimental proof of resonant tunneling involving X states was provided by Mendez et al. in GaAs-$Ga_{0.60}Al_{0.40}As$ double-barriers [19] and, more recently, in GaAs-AlAs [20]. Figure 7 shows the I-V characteristic of a $Ga_{0.60}Al_{0.40}As$-GaAs-$Ga_{0.60}Al_{0.40}As$ heterostructure, up to high bias. Below 0.5V two negative-resistance features are identified with resonant tunneling via the bound states of the GaAs well. A weaker structure at ~0.9V is attributed to tunneling via the $Ga_{0.60}Al_{0.40}As$ X state, as illustrated in the inset of Fig.7. Effective-mass calculations for the transmission probability are in good agreement with the observations. It is to be noted that the effective mass of the electron along this tunneling path is very heavy (of the order of m_0), in contrast with the inelastic paths discussed above.

In samples in which the Al content in $Ga_{1-x}Al_xAs$ is considerably smaller than x~0.40, no features related to X have been observed. This is understandable, since for those compositions the X point would have an energy significantly larger than Γ and therefore the large non-resonant current background at high bias would hide the X resonance. On the contrary, in AlAs X is ~0.8eV below Γ and that background should be absent. The X resonance is clearly visible in 50Å-50Å-50Å AlAs-GaAs-AlAs structures, as shown on Fig.8. An additional large contribution to the current, originating from non-resonant tunneling through the X_y and X_z ellipsoids is also observable.

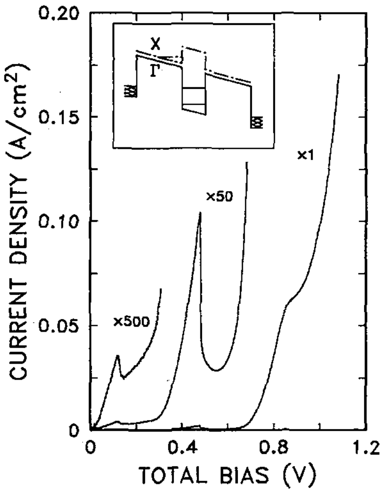

Fig.7.- I-V characteristic at 4K for the DBH described in the Fig.4 caption, at p=0. The feature at ~0.9V, corresponds to resonant tunneling via a state confined in GaAlAs by an X-point potential profile, sketched in the inset. (After Ref. [19].)

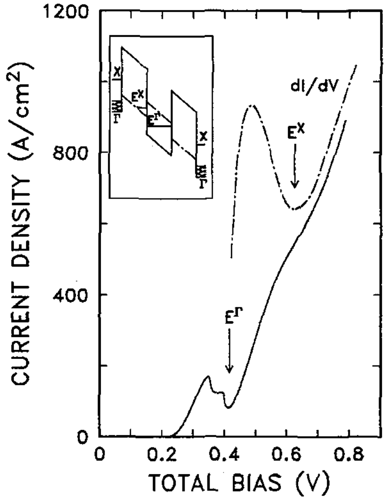

Fig.8.- I-V characteristic for a GaAs-AlAs DBH with 50Å layer widths. A weak structure at ~0.55V, better resolved in conductance measurements, is attributed to resonant tunneling via an X-point AlAs state. Data taken at 4K. (After Ref. [20].)

When the thickness of the GaAs layer is >30Å the ground state of the system, under flat-band conditions, has a Γ character, and is localized in GaAs. On the other hand, if that thickness is <30Å the ground state is confined in AlAs and is X in nature. Moreover, a confined X state is formed even when a single AlAs layer is clad between GaAs electrodes. Recent experiments in both kinds of structures have confirmed these hypotheses [20].

5. Conclusion

I have reviewed some of the advances reported in the last two years in the physics of resonant tunneling. They have helped us to understand better the nature of the process and of the potential that controls the tunneling current. They have also pointed the limitations of a simple one-dimensional, one-band, model and the need of more realistic calculations that take into account the band structure of the materials involved. In their absence we are forced to take naïve simplifications, like the one used here of artificially separating Γ and X profiles.

Another topic which needs more study is the dichotomy of sequential and resonant tunneling. As stated clearly by Luryi [24], the presence of negative resistance in the I-V characteristic is no direct proof that the electronic wavefunction remains coherent during the whole tunneling process. A two-step process, in which the electron hops from one electrode to another, tunneling sequentially through the barriers via an intermediate quantum state, can also give rise to negative resistance. The intuitive view that the amount of current would be smaller in sequential tunneling than in coherent tunneling, has been recently disputed by a report asserting the equivalency of both mechanisms in terms of the final tunnel current [25]. Theoretical calculations that include inelastic scattering, as well as more systematic experiments, are needed before this conceptual problem is fully solved.

6. Acknowledgements

The work reviewed in detail here has been done in collaboration with E. Calleja, L. L. Chang, L. Esaki, C. E. T. Gonçalves da Silva, and W. I. Wang, and it has been sponsored in part by the Army Research Office.

7. References

/1/ See, e.g., Gundlach, K. H., *Solid State Electron.* **9** (1966) 949.
/2/ Duke, C. B., *Tunneling in Solids*, p.79, (Academic Press, New York) 1969.
/3/ Chang, L. L., Esaki, L. and Tsu, R., *Appl. Phys. Lett.* **24** (1974) 593.
/4/ Sollner, T. C. L. G., Goodhue, W. D., Tannenwald, P. E., Parker, C. D. and Peck D. D., *Appl. Phys. Lett.* **43** (1983) 588.
/5/ Mendez, E. E., Wang, W. I., Ricco, B. and Esaki, L., *Appl. Phys. Lett.* **47** (1985) 415.
/6/ Nakagawa, T., Imamoto, H., Kojima, T. and Ohta, K., *Appl. Phys. Lett.* **49** (1986) 73.
/7/ Nakagawa, T., Fujita, T., Matsumoto, Y., Kojima, T. and Ohta, K., *Appl. Phys. Lett.* **50** (1987) 974.
/8/ Capasso, F., Mohammed, K. and Cho, A. Y., *Appl. Phys. Lett.* **48** (1986) 478.
/9/ Esaki, L. and Chang, L. L., *Phys. Rev. Lett.* **33** (1974) 495.
/10/ Davies, R. A., Kelly, M. J. and Kerr, T. M., *Phys. Rev. Lett.* **55** (1985) 1114.
/11/ Gavrilovic, P., Brown, J. M., Kaliski, R. W., Holonyak, Jr., N., Hess, K., Ludowise, M. J., Dietze, W. T. and Lewis, C. R., *Solid State Commun.* **52**, (1984) 237.
/12/ Vuong, T. H. H., Tsui, D. C. and Tsang, W. T., *Appl. Phys. Lett.* **50** (1987) 212.
/13/ Reed, M. A., Koestner, R. J. and Goodwin, M. W., *Appl. Phys. Lett.* **49** (1986) 1293.
/14/ Sollner, T. C. L. G., Tannenwald, P. E., Peck D. D. and Goodhue, W. D., *Appl. Phys. Lett.* **45** (1984) 1319.
/15/ Yokoyama, N., Imamura, K., Muto, S., Hiyamizu, S. and Nishi, H., *Japan J. Appl. Phys.* **24** (1985) L583.
/16/ Capasso, F., Sen, S., Gossard. A. C., Hutchinson, A. L. and English, J. H., *IEEE Electron Device Lett.* **EDL-7** (1986) 573.
/17/ Mendez, E. E., Esaki, L. and Wang, W. I., *Phys. Rev. B* **33** (1986) 2893.
/18/ Mendez, E. E., Calleja, E. and Wang, W. I., *Phys. Rev. B* **34** (1986) 6026.
/19/ Mendez, E. E., Calleja E., Gonçalves da Silva, C. E. T., Chang L. L. and Wang, W. I., *Phys. Rev. B* **33** (1986) 7368.
/20/ Mendez E. E., Wang, W. I., Calleja E. and Gonçalves da Silva, C. E. T., *Appl. Phys. Lett.* **50** (1987) 1263.
/21/ Goldman, V. J., Tsui, D. C. and Cunningham, J. E., *Phys. Rev. B* **35** (1987) xxxx.
/22/ Blakemore, J. S., *J. Appl. Phys.* **53** (1982) R123.
/23/ Finkman, E., Sturge, M. D. and Tamargo, M. C., *Appl. Phys. Lett.* **49** (1986) 1299.
/24/ Luryi, S., *Appl. Phys. Lett.* **47** (1985) 490.
/25/ Weil, T. and Vinter, B., *Appl. Phys. Lett.* **50** (1987) 1281.